Bioorganic & Medicinal Chemistry 19 (2011) 414–421

Contents lists available at ScienceDirect

Bioorganic & Medicinal Chemistry

journal homepage: www.elsevier.com/locate/bmc

NF kappa B inhibitors and antitrypanosomal metabolites from endophytic fungus *Penicillium* sp. isolated from *Limonium tubiflorum*

Amal H. Aly [a,*], Abdessamad Debbab [a], Carol Clements [b], RuAngelie Edrada-Ebel [b], Barbora Orlikova [c], Marc Diederich [c], Victor Wray [d], WenHan Lin [e], Peter Proksch [a,*]

[a] Heinrich-Heine-Universität, Institut für Pharmazeutische Biologie und Biotechnologie, Universitätsstrasse 1, Geb. 26.23, D-40225 Düsseldorf, Germany
[b] Strathclyde Institute of Pharmacy and Biomedical Science, University of Strathclyde, The John Arbuthnott Building, 27 Taylor Street, Glasgow G4 0NR, UK
[c] Laboratoire de Biologie Moléculaire et Cellulaire du Cancer, Hôpital Kirchberg 9, rue Steichen L-2540, Luxembourg
[d] Helmholtz Centre for Infection Research, Inhoffenstraße 7, D-38124 Braunschweig, Germany
[e] National Research Laboratories of Natural and Biomimetic Drugs, Peking University, Health Science Center, 100083 Beijing, People's Republic of China

ARTICLE INFO

Article history:
Received 14 September 2010
Accepted 5 November 2010
Available online 17 November 2010

Keywords:
Penicillium
Limonium tubiflorum
Endophytic fungi
Natural products
Trypanosoma
Antitrypanosomal activity
Cytotoxic activity
NF kappa B

ABSTRACT

Chemical investigation of the endophytic fungus *Penicillium* sp. isolated from *Limonium tubiflorum* growing in Egypt afforded four new compounds of polyketide origin, including two macrolides, penilactone (**1**) and 10,11-epoxycurvularin (**2**), a dianthrone, neobulgarone G (**7**), and a sulfinylcoumarin, sulfimarin (**14**), along with twelve known metabolites (**3**–**6**, **8**–**13**, **15** and **16**). The structures of all compounds were assigned by comprehensive spectral analysis (1D and 2D NMR) and mass spectrometry. Compounds **3**, **4**, **13** and **16** showed pronounced antitrypanosomal activity with mean MIC values ranging from 4.96 to 9.75 μM. Moreover, when tested against a panel of three human tumor cell lines compounds **3**, **4**, **6** and **12** showed selective growth inhibition against Jurkat and U937 cell lines with IC_{50} values ranging from 1.8 to 13.3 μM. The latter compounds also inhibited TNFα-induced NF-κB activity in K562 cells with IC_{50} values ranging from 1.6 to 10.1 μM, respectively.

1. Introduction

African trypanosomiasis (also known as sleeping sickness) is an important chronic disease which affects wild and domestic animals as well as humans. It is caused by the parasitic protozoan, *Trypanosoma brucei*, a single-cell flagellate which is transmitted by arthropod vectors and survives extracellularly in the blood and tissues of the host.[1,2] During the last few decades, an alarming reemergence of this neglected disease, mostly affecting poor and marginalised populations, was observed in sub-Saharan Africa.[3] The treatment regimen depends on the stage of the disease, in early stages the probability of cure is higher and administered drugs are less toxic and more effective. However, due to undesired side effects the search for new drugs and eventually new drug targets is necessary. Furthermore, trypanosomes, including *Trypanosoma brucei*, are eukaryotes that show specific biochemical peculiarity.[2] They are able to evade their host immune response mainly by antigenic variation,[1] a fact that inhibited efforts to develop and design new effective drugs and vaccines against this disease. Thus, attention should be drawn towards this neglected disease to improve its control by drug development and vector elimination.

Recent studies showed that chronic inflammation might be crucial in contributing to inflammation-associated cancer.[4,5] Tumor necrosis factor alpha (TNFα) is a potent proinflammatory cytokine that activates signaling pathways, including nuclear factor kappa B (NF-κB) activation pathway, to elicit a specific gene expression program.[6] Target genes of the NF-κB-activation pathway are known to regulate diverse cellular processes including inflammation, immune response, differentiation, proliferation, apoptosis and cancer.[5–7] NF-κB is inactive in resting cells, but cytokine signaling, innate or adaptive immune responses, or environmental stress can initiate its activation.[8] In recent studies, the role of NF-κB-activation pathway in acute inflammation and cell-survival, as well as its sustained activation in several cancer cases has been reported, thereby linking inflammation to tumor promotion and progression.[4,9] In many cases inflammatory processes are important determinants of tumor development,[5] in some cases even at the stage of initiation (e.g., *Helicobacter*-induced gastric cancer).[10] On the other hand, chemicals with known chemopreventive properties (e.g., natural products, such as ginseng extract, green-tea extract, resveratrol and curcumin) can interfere with NF-κB

* Corresponding authors. Tel.: +49 211 81 14163; fax: +49 211 81 11923 (P.P.).
E-mail addresses: amal.hassan@uni-duesseldorf.de (A.H. Aly), proksch@uni-duesseldorf.de (P. Proksch).

0968-0896/$ - see front matter © 2010 Elsevier Ltd. All rights reserved.
doi:10.1016/j.bmc.2010.11.012

activation and thus reduce cancer incidence.[11] Hence, targeting NF-κB in chronic inflammatory diseases is of great potential in cancer prevention.

In the search for new effective drugs fungal endophytes have continuously proven to be a promising resource of unique metabolites with great pharmacological potential.[12–14] Endophytic fungi spend the whole or part of their life cycle colonizing healthy tissues of their host plants, typically causing no apparent symptoms of disease.[15] This colonization is believed to contribute to host plant adaptation to biotic and abiotic stress factors,[16–18] which in many cases has been correlated with fungal natural products.[14] Hence, there are numerous examples of endophytes producing secondary metabolites with pharmaceutical or agricultural potential. For example, guanacastepenes, produced by an unidentified endophytic fungus isolated from the tree *Daphnopsis americana*, exhibited pronounced antibiotic activity against drug-resistant *Staphylococcus aureus* and *Enterococcus faecium*.[19] Potent antimycotic activity was reported for cryptocandin A obtained from endophytic *Cryptosporiopsis quercina*.[20,21] Chaetomellic acids A and B, isolated from endophytic *Chaetomella acutisea*, were found to disrupt Ras-dependent proliferative activity by specifically inhibiting farnesyl-protein transferase.[22] Furthermore, a potential chemical control agent for rice blast, cryptocin, is produced by endophytic *Cryptosporiopsis quercina* and shows potent activity against *Pyricularia oryzae*.[23]

Penicillium is a genus of ascomycetous fungi of great importance in the environment as well as in drug discovery. It was the source of the first antibiotic, penicillin G, discovered by Alexander Fleming from *Penicillium notatum* almost 90 years ago (1928). Since then fungal microorganisms, including members of the genus *Penicillium*, have been the subject of intensive studies to unveil the treasures of their secondary metabolites.[24,25] In the course of our continued studies on endophytic fungi for bioactive natural products,[26–29] a crude EtOAc extract obtained from *Penicillium* sp. (Trichocomaceae) isolated from stem tissues of *Limonium tubiflorum* (Rutaceae) showed significant cytotoxic activity (reduction of cellular growth by 90% at a dose of 10 μg/mL measured by MTT assay) against murine L5178Y cells which served as an initial screen. This stimulated our investigation of the metabolites of this fungal endophyte as well as of their biological activities in several cell based bioassays employing trypanosomes and various cancer cell lines as well as the molecular target NF-κB which is of relevance for treatment of cancer and inflammatory diseases.

2. Results and discussion

The crude EtOAc extract of *Penicillium* sp. when grown on solid rice medium was partitioned between *n*-hexane and 90% aqueous MeOH. Fractionation of the 90% aqueous MeOH phase by vacuum liquid chromatography (VLC) on silica gel, followed by size exclusion chromatography over Sephadex LH-20 and preparative reversed-phase HPLC yielded four new metabolites, including two macrolides, penilactone (**1**) and epoxycurvularin (**2**), a dianthrone, neobulgarone G (**7**), and a sulfinylcoumarin, sulfimarin (**14**), in addition to twelve known compounds (**3**–**6**, **8**–**13**, **15** and **16**, Fig. 1).

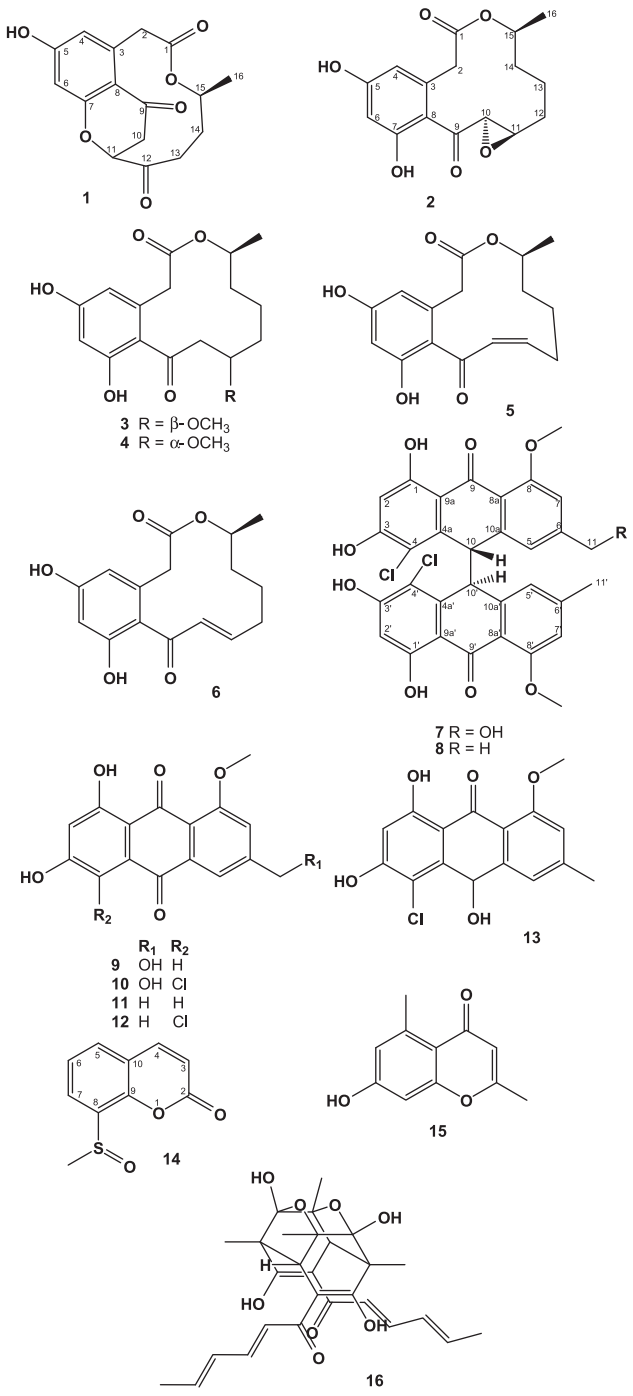

Figure 1. Chemical structures of compounds **1**–**16**.

ESIMS indicated a molecular weight of 304 g/mol for compound **1**. Its molecular formula was determined as $C_{16}H_{16}O_6$, on the basis of the $[M+H]^+$ signal at *m*/*z* 306.1078 (corresponding to $C_{16}H_{16}DO_6$ due to deuterium exchange) in the HRESIMS indicating nine elements of unsaturation. Inspection of the ^1H and ^{13}C NMR spectra of **1** (Table 1) revealed the presence of a pair of *meta*-coupled aromatic protons both appearing at δ_H 6.30 ppm (H-4 and H-6), four methylene groups (CH_2-2 at δ_H 4.10 and 3.50 ppm, CH_2-10 at 3.12 and 2.79 ppm, CH_2-13 at 2.47 ppm, and CH_2-14 at 1.85 and 1.46 ppm), two oxygenated methine groups at δ_H 4.90 (δ_C 84.1) and δ_H 4.62 (δ_C 74.2) ppm (CH-11 and -15, respectively), and a methyl group (CH_3-16) resonating at δ_H 1.09 ppm. Furthermore, ^{13}C NMR and DEPT spectra disclosed signals for seven sp^2 quaternary carbons, of which two were attributed to the carbonyl groups at C-9 and C-12 (δ_c 199.7 and 207.1 ppm, respectively), one to the ester carbonyl group at C-1 (δ_c 171.3 ppm), and four to the aromatic carbons (C-3, C-5, C-7 and C-8). The deshielded signals for C-5 and C-7 (δ_C 177.7 and 170.3 ppm, respectively) indicated their oxygenated nature.

Inspection of the COSY and HMBC spectra (Table 1) revealed the presence of a continuous spin system beginning with CH_2-13 to CH_3-16. The downfield chemical shift of CH_2-13 (δ_H 2.47 ppm) indicated

Table 1
NMR spectroscopic data of **1** at 600 (^{1}H) and 150 (^{13}C) MHz in MeOH-d_4 (δ in ppm, mult., J in Hz)

Position	δ_H	COSY	HMBC	δ_C
1				171.3
2	A 4.10, d (17.7)	2B, 4	1, 3, 4, 8	39.6
	B 3.50, d (17.7)	2A, 4		
3				137.4
4	6.30, s	2A/B	2, 5, 6, 8, 9	115.0
5				177.7
6	6.30, s		4, 5, 7, 8, 9	98.0
7				170.3
8				113.3
9				199.7
10	A 3.12, dd (12.9, 4.4)	10B, 11	9, 11, 12	44.2
	B 2.79, dd (13.2, 4.4)	10A, 11		
11	4.90, dd (4.4, 4.1)	10A/B		84.1
12				207.1
13	2.47, m	14A/B	12, 14, 15	42.3
14	A 1.85, m	13, 14B	12, 13, 15, 16	27.6
	B 1.46, m	13, 14A		
15	4.62, m	14A/B, 16		74.2
16	1.09, d (6.0)	15	14, 15	20.5

Table 2
NMR spectroscopic data of **2** at 500 (^{1}H) and 125 (^{13}C) MHz in MeOH-d_4 (δ in ppm, mult., J in Hz)

Position	δ_H	COSY	HMBC	δ_C[a]
1				172.8
2	A 3.87, d (15.8)	2B, 4	1, 3, 4, 8	40.0
	B 3.37, d (15.8)	2A, 4		
3				136.1
4	6.20, d (2.2)	2A/B, 6	2, 5, 6, 8	111.8
5				162.1
6	6.27, d (2.2)	4	7, 8	102.1
7				159.9
8				120.0
9				203.9
10	4.08, d (1.9)	11	9, 11	61.9
11	2.94, ddd (9.8, 2.8, 2.2)	10, 12A/B		63.8
12	A 2.08, m	11, 12B, 13, 14A/B		32.8
	B 1.16, m	11, 12A, 13, 14A/B		
13	1.60, m	12A/B, 14A/B		21.5
14	A 1.76, m	12A/B, 13, 14B, 15		34.0
	B 1.58, m	13, 14A, 15		
15	4.82, m	14A/B, 16		74.1
16	1.03, d (6.3)	15	14, 15	19.0

[a] Derived from HMQC and HMBC spectra.

its position adjacent to a carbonyl function. This was further confirmed by the HMBC correlations of CH_2-13 and -14 to the carbonyl group at C-12. Moreover, CH_2-10 showed COSY correlations with CH-11, as well as HMBC correlations to both carbonyl groups at C-9 and C-12. These correlations established the connection between the fragment CH_2(10)CH(11) to C-9 and C-12. Diagnostic HMBC correlations of CH_2-2 to C-1, C-3, C-4, and C-8, as well as of H-6 to C-4, C-5, C-7 and C-8 revealed the phenylacetic acid substructure of **1**. Furthermore, the observed HMBC correlations of H-4 and H-6 to C-9 due to the 4-bond couplings established the connection of the carbonyl group to the aromatic ring. The linkage between C-1 and the oxygenated methine group at C-15 via an ester bond was deduced by comparison with NMR data of related compounds such as curvularin and dehydrocurvularin (**6**)[30–32] as well as apralactone A.[33] Finally, connecting the oxygenated aromatic carbon C-7 and CH-11 to form a common 4-chromanone ring system rationalized the remaining element of unsaturation. It is worth mentioning that the incorporation of 4-chromanone moieties in macrolactone rings is rather rare among macrolides. Thus, compound **1** was identified as the new natural product penilactone. The configuration of **1** at C-15 was assumed to be *S*, by comparison of its $[\alpha]_D$ value with those of similarly configured curvularin-type metabolites as well as of their enantiomers.[33]

The molecular formula of **2** was determined as $C_{16}H_{18}O_6$, on the basis of the $[M+Na]^+$ signal at *m/z* 329.0999 in the HRESIMS, thus revealing an increase in the molecular weight of 2 amu compared to **1**. ^{1}H NMR, COSY and HMBC spectra of **2** (Table 2) indicated a pair of *meta*-coupled aromatic protons, appearing at δ_H 6.27 and 6.20 ppm (H-6 and H-4, respectively), and an isolated methylene group resonating at δ_H 3.87 and 3.37 ppm (CH_2-2), which were comparable to the respective signals of metabolite **1**. In addition, the spectrum of **2** contained an extended aliphatic spin system, which due to a significant degree of overlap could only be completely assembled with the help of a COSY spectrum. It included an aliphatic methyl group (CH_3-16) adjacent to an oxygenated methine group (δ_H 4.82 ppm, CH-15). The latter was further connected to a chain of methylene groups (CH_2-14, CH_2-13 and CH_2-12), appearing as a complex set of multiplets resonating between 1.13 and 2.10 ppm, which are all familiar features from related curvularin derivatives,[30–32] except for the attachment of the last methylene group in the chain (CH_2-12) to an oxygenated methine group resonating at δ_H 2.94 ppm (CH-11) which was attached to a further oxygenated methine group (CH-10) resonating at δ_H 4.08 ppm. The ^{13}C NMR chemical shifts of both oxymethine groups (δ_C 61.9 and 63.8 ppm) were diagnostic for the presence of a 1,2-disubstituted epoxide.[34]

The downfield chemical shift of CH-10 (δ_H 4.08 ppm) indicated it was an α-position to a carbonyl function at C-9, whereas the β-position of CH-11 was concluded from its upfield chemical shift (δ_H 2.94 ppm). This was further confirmed by the HMBC correlation of CH-10 to the carbonyl group at C-9. The relative stereochemistry of the epoxide group was established as *trans* by analysis of the ^{1}H–^{1}H coupling constants and comparison with data from related compounds.[31,34] *Trans* configurated epoxide rings show smaller coupling constants than *cis*-configurated ones[34] and indicated the observed value of 1.9 Hz belonged to a *trans* system.

The phenylacetic acid substructure of **2** was concluded from diagnostic correlations of CH_2-2 to C-1, C-3, C-4, and C-8, of H-4 to C-5, C-6 and C-8, as well as of H-6 to C-7 and C-8 in analogy to **1**. Similar to **1** and related curvularin derivatives[30–33] an ester bond connected C-1 to the oxygenated methine group at C-15. Thus, compound **2** was identified as the new natural product 10,11-epoxycurvularin. By analogy with **1**, the *S*-configuration was assumed at C-15 based on the measured $[\alpha]_D$ value.[33]

The $[M+H]^+$ signal at *m/z* 623.0866 in the HRESIMS of **7** indicated a molecular formula of $C_{32}H_{24}Cl_2O_9$. The isotope patterns of the molecular ions observed in the recorded mass spectrum indicated the presence of two chlorine atoms in the molecule. Partial fragmentation of the compound was observed in the ESIMS experiment where **7** yielded fragments at *m/z* 304 and 320 indicating that the compound was composed of two monomers with molecular weights of 303 and 319 g/mol. Furthermore, ^{1}H NMR and COSY spectra (Table 3) showed two almost identical sets of signals thus confirming that the compound was an asymmetrical dimer consisting of two structurally closely related monomers. The signals due to one half of the dimer were identical to the signals recorded for compound **8** (neobulgarone E),[35] a symmetrical dimer composed of two moieties of 5-chloro-6,8-dihydroxy-1-methoxy-3-methyl-9(10*H*)-anthracenone. Signals attributed to this substructure included a pair of *meta*-coupled aromatic protons appearing at δ_H 6.85 and 5.59 ppm (H-7′ and H-5′), one aromatic proton singlet at δ_H 6.41 ppm (H-2′), one methine group at δ_H 4.99 ppm (CH-10′), two phenolic hydroxyl groups at δ_H 12.70 and 11.38 ppm (1′- and 3′-OH, respectively), one of which is chelated (1′-OH), a methoxyl group at δ_H 3.71 ppm (8′-OCH_3), and one methyl group at δ_H 2.06 ppm (CH_3-11′). In contrast, signals due to the other half of the molecule were slightly shifted downfield.

Table 3
NMR spectroscopic data of **7** at 500 (^{1}H) and 125 (^{13}C) MHz in DMSO-d_6 (δ in ppm, mult., J in Hz)

Position	δ_H	COSY	HMBC	δ_C[a]
1				161.1
2	6.44, s		1, 3, 4, 9a	101.7
3				158.1
4				110.5
4a				138.0
5	5.71, br s	7, 11	7, 8a, 10, 11	119.3
6				
7	6.97, br s	5, 11	5, 8a, 11	113.6
8				158.9
8a				119.3
9				
9a				113.2
10	5.02, d (5.4)		4, 4a, 5, 8a, 9a, 10a, 10′	48.0
10a				138.0
11	4.23, d (4.8)	5, 7, 11-OH	5	61.4
8-OCH_3	3.73, s	7	8	56.5
1-OH	12.73, s		1, 2, 9a	
3-OH	11.42, s			
11-OH	5.23, t (5.7)	11		
1′				161.1
2′	6.41, s		1′, 3′, 4′, 9a′	101.2
3′				158.0
4′				110.5
4a′				138.0
5′	5.59, br s	7′, 11′	7′, 8a′, 10′, 11′	122.4
6′				143.2
7′	6.85, br s	5′, 11′	5′, 8a′, 11′	109.8
8′				158.9
8a′				118.5
9′				
9a′				113.1
10′	4.99, d (5.4)		4′, 4a′, 5′, 8a′, 9a′, 10a′, 10	48.0
10a′				138.0
11′	2.06, s	5′, 7′	5′, 6′, 7′	21.0
8′-OCH_3	3.71, s	7′	8′	56.5
1′-OH	12.70, s		1′, 2′, 9a′	
3′-OH	11.38, s			

[a] Derived from HMBC spectra.

They included similar signals for three aromatic protons (δ_H 6.97, 6.44 and 5.71 ppm corresponding to H-7, -2 and -5, respectively), two phenolic hydroxyl groups (1- and 3-OH at δ_H 12.73 and 11.42 ppm, respectively), one methine group (CH-10 at δ_H 5.02 ppm), and a methoxyl group (8-OCH_3 at δ_H 3.73 ppm). However, the methyl group signal of the first monomer was replaced by a methylene group resonating at δ_H 4.23 (CH_2-11) which correlated with an aliphatic hydroxyl group at δ_H 5.23 (11-OH), thereby explaining the asymmetry of **7** compared to structurally related symmetrical dimers such as neobulgarone E.

The structure of **7** was further confirmed by interpretation of the HMBC spectra (Table 3). The dimeric nature of the compound was corroborated by the observed HMBC correlation from H-10 to C-10′ (and vice versa from H-10′ to C-10). H-10 gave further HMBC correlations to C-4, C-4a, C-5, C-8a, C-9a, and C-10a. The structure of one aromatic ring was established by the correlations of H-2 to C-1, C-3, C-4, and C-9a. The other ring was deduced from correlations of H-5 to C-7, C-8a, C-10, and C-11, as well as by those of H-7 to C-5, C-8a, and C-11. Likewise, H-2′, H-5′, H-7′and H-10′ gave similar HMBC correlations which all together established the structure of **7**. Thus, compound **7** was identified as the new natural product neobulgarone G.

In order to establish the relative stereochemistry of **7**, the $[\alpha]_D$ value was measured and compared to that of **8**. Although previously isolated,[35] no attempts were made to determine the relative stereochemistry of **8**. As it is a symmetrical dimer, the optical activity of **8** ($[\alpha]_D^{20} = -77$, c 0.025, acetone) indicated a *syn* relationship between H-10 and H-10′. In contrast, related *meso*-stereoisomers are reported to be optically inactive.[36,37] Based on the $[\alpha]_D$ values, compound **7** was assumed to have a similar configuration at C-10 and C-10′. Furthermore, ^{1}H–^{1}H coupling constants were calculated and compared with data from related compounds. Thus, a coupling constant of 5.4 Hz between H-10 and H-10′ indicated the *syn* relationship of these protons.[37]

The molecular formula of **14** was determined as $C_{10}H_8O_3S$, on the basis of the $[M+H]^+$ signal at m/z 209.0266 in the HRESIMS. Inspection of the proton chemical shifts in the ^{1}H NMR spectrum (Table 4) indicated a monosubstituted coumarin structure.[38] Interpretation of the ^{1}H and ^{13}C NMR spectra of **14** (Table 4) in combination with COSY data revealed the presence of a pair of *ortho*-coupled aromatic protons at δ_H 8.13 and 6.58 ppm (H-4 and H-3, respectively), an aromatic ABC system observed at δ_H 7.91, 7.88 and 7.59 ppm (H-7, H-5 and H-6, respectively), in addition to a methyl group at δ_H 2.86 (δ_C 41.5) ppm. Furthermore, the ^{13}C NMR spectrum disclosed signals for four sp^2 quaternary carbons, of which three were assigned to the aromatic carbons (C-8, C-9, and C-10), while the remaining one was attributed to the ester carbonyl group at C-2 (δ_c 158.0 ppm).

The coumarin structure of **14** was further confirmed by inspection of the HMBC spectrum showing correlations of H-3 to C-2 and C-10, of H-4 to C-2, C-5, and C-9, of H-5 to C-4, C-7, and C-9, of H-6 to C-8 and C-10, and of H-7 to C-5 and C-9. The downfield chemical shifts of the methyl group at δ_H 2.86 (δ_C 41.5 ppm) and the presence of one sulfur atom in the molecule suggested the attachment of the methyl group to a sulfoxide function located at C-8.[39] Moreover, the signal for C-8 (δ_C 133.0 ppm) was likewise shifted downfield compared to those of unsubstituted coumarins.[40–42] This was further confirmed by the single HMBC correlation observed for the methyl group to C-8, as well as the MS/MS fragments at m/z 193.9 $[M+H-CH_3]^+$ and 146.1 $[M+H-SOCH_3]^+$. Thus, **14** was identified as the new natural product sulfimarin.

The remaining compounds (**3**–**6**, **8**–**13**, **15** and **16**) were identified on the basis of their ^{1}H NMR, ^{13}C NMR, and mass spectrometric data and comparison with published data as 11β-methoxycurvularin (**3**),[43] 11α-methoxycurvularin (**4**),[43] *cis*-dehydrocurvularin (**5**),[31] *trans*-dehydrocurvularin (**6**),[31] neobulgarone E (**8**),[35] carviolin (**9**),[44] 5-chloro-ω-hydroxy-1-*O*-methylemodin (**10**),[45] 1-*O*-methylemodin (**11**),[46] 1-chloro-2,4-dihydroxy-5-methoxy-7-methylanthraquinone (**12**),[46] 5-chloro-6,8,10-trihydroxy-1-methoxy-3-methyl-9(10*H*)-anthracenone (**13**),[46] 2,5-dimethyl-7-hydroxychromone (**15**),[47] and trichodimerol (**16**).[48]

The isolated compounds were evaluated for their antitrypanosomal activities. Selected compounds were also tested for cytotoxicity and NF-κB inhibition. Compounds **3**, **4**, **13** and **16** showed pronounced antitrypanosomal activity with MIC values of 4.96, 9.68, 9.75, and 6.29 μM, respectively (Table 5). These results indicated that 11β-methoxycurvularin (**3**) was the most potent of the tested compounds. Interestingly, a change in the stereochemistry of the methoxyl group in 11α-methoxycurvularin (**4**) resulted in a decrease of activity by a factor of two. The lack of activity of the remaining curvularin derivatives in the antitrypan-

Table 4
NMR spectroscopic data of **14** at 500 (^{1}H) and 125 (^{13}C) MHz in DMSO-d_6 (δ in ppm, mult., J in Hz)

Position	δ_H	COSY	HMBC	δ_C
2				158.0
3	6.58, d (9.8)	4	2, 10	117.0
4	8.13, d (9.5)	3	2, 5, 9	143.9
5	7.88, dd (7.7, 1.6)	6	4, 7, 9	130.8
6	7.59, t (7.7)	5, 7	8, 10	125.0
7	7.91, dd (7.7, 1.6)	6	5, 9	126.2
8				133.0
9				149.0
10				119.0
CH_3	2.86, s		8	41.5

Table 5
Antitrypanosomal activity of isolated compounds[a]

Compound	MIC (μM)
2	>100
3	4.96
4	9.68
5	>100
6	>100
7	>100
8	>100
9	41.66
10	18.71
11	10.98
12	78.61
13	9.75
14	>100
15	>100
16	6.29
Agelasine D	14.8
Suramin	0.06

[a] Compounds considered active when MIC <10 μM.

osomal assay indicated that changes in the conformation of the macrolide ring, as in **2**, **5** and **6**, may eliminate antiprotozoal activity. Trichodimerol (**16**) was the next most active compound followed by the anthraquinone derivative **13**. The planar structure of the anthraquinone derivatives **9**–**12** as well as the dimeric nature of compounds **7** and **8** may account for their inactivity.

Additionally, the compounds were tested against a panel of human tumor cell lines, including human Philadelphia chromosome-positive chronic myelogenous leukemia cells (K562), human T cell leukemia cells (Jurkat) and human histiocytic lymphoma cells (U937), to evaluate their in vitro inhibitory activity and subsequently their cytotoxic activity using the CellTiter-Glo® Luminescent Cell Viability Assay. The results showed that compounds **3**, **4** and **6** selectively inhibited the growth of Jurkat cells (IC_{50} = 3.9, 2.3, and 5.5 μM, respectively), whereas **3**, **4**, **6** and **12** were active against U937 cells (IC_{50} = 1.8, 4.6, 2.5, and 7.6 μM, respectively) (Table 6). In contrast, all compounds showed only weak activity against K562 cells with IC_{50} values >10 μM. Hence, in comparison to other anthraquinone derivatives tested in this study, **12** was the most active against all three cell lines. The weaker activity of **10** indicated that the presence of a free methyl group is essential for cytotoxic activity. Another crucial component appears to be the chlorine substituent, as assumed from the lack of activity of **11**. Accordingly **9**, lacking both a free methyl group and a chlorine substituent, was inactive in the assay. Similarly **7**, having only one free methyl group, was less active than **8**. Although bearing chlorine substituents, the lack of activity of **7** and **8** may be due to their dimeric nature.

Table 6
Effect of tested compounds on cell viability and their inhibition potential on TNFα-induced NF-κB activity in K562 cell line expressed in terms of IC_{50} values[a]

Compound	Effect on cell viability			Inhibition of NF-κB activity
	K562	Jurkat	U937	
3	12.4 ± 1.0	3.9 ± 0.4	1.8 ± 0.4	4.7 ± 0.6
4	41.1 ± 5.3	2.3 ± 0.1	4.6 ± 1.0	10.1 ± 0.5
6	37.0 ± 7.1	5.5 ± 0.3	2.5 ± 0.3	5.6 ± 0.8
7	Non toxic	>100	>100	>100
8	>100	82.4 ± 5.2	47.6 ± 3.3	46.0 ± 8.8
9	Non toxic	>100	>100	>100
10	40.1 ± 4.4	28.4 ± 0.4	22.0 ± 2.0	16.0 ± 2.5
11	Non toxic	>100	88.6 ± 5.0	>100
12	24.8 ± 3.0	13.3 ± 0.4	7.6 ± 1.1	1.6 ± 0.6
16	74.4 ± 7.0	28.5 ± 2.8	16.5 ± 2.0	47.8 ± 7.4

[a] IC_{50} values are listed in μM. Compounds considered active when IC_{50} <10 μM. An average value of three independent experiments is reported.

A well known tumor progression mechanism involves the activation of the transcription factor NF-κB which leads to gene expression regulating processes engaged in immune responses, inflammation, and cell survival.[7] Since the tumor necrosis factor alpha (TNFα) is known to activate NF-κB through a definite kinase pathway, the compounds were examined for their effect on TNFα-induced NF-κB activity in K562 cells. This was performed using a luciferase reporter gene assay, which allowed measurement of two independent expression vectors simultaneously within one sample. Compounds **3**, **4**, **6** and **12** significantly reduced TNFα-induced NF-κB activation as expressed by their IC_{50} values of 4.7, 10.1, 5.6, and 1.6 μM, respectively. The concentration necessary to decrease cell viability to about 50% was significantly higher than the concentration at which 50% of NF-κB activity was abolished. Hence, we would like to stress that NF-κB inhibition potential of active compounds in K562 cell line was reached at a concentration, which was lower than the concentration responsible for cytotoxic effects, thereby cytotoxicity is not primarily responsible for the observed NF-κB inhibition activity.

Obviously, two other cell lines (Jurkat, U937) were more sensitive when exposed to the tested compounds and the ATP metabolism was negatively impacted at much lower concentrations. Hence, the cytotoxic effect was reached at lower concentrations. These results may indicate the involvement of the tested compounds in cell death mechanisms, which was not examined in detail. Thus, inhibition of the NF-κB pathway by fungal metabolites **3**, **4**, **6** and **12** could be contributing to the observed cytotoxic effects of the respective compounds against cancer cells (Table 6).

Our findings confirm the results of He et al. concerning the cytotoxicity of 11-methoxycurvularin and dehydroculvularin in four different cancer cells lines.[49] In case of 11-methoxycurvularin we distinguish between *alpha* and *beta*-isoforms of the same compound. With both 11-methoxycurvularins and dehydroculvularin we reached a comparable IC_{50} for the U937 histiocytic lymphoma. Compound **12** was not described to have cytotoxic potential as yet. Interestingly, none of these investigated anthraquinones were described to inhibit NF-κB and may thus provide potential leads for future investigation.

Several studies reported activation of NF-κB and its downstream targets upon *Trypanosoma cruzi* infection.[50–53] Huang et al. demonstrated that the activation of NF-κB pathway in endothelial cells associated with *T. cruzi* infection may be an important factor in the inflammatory response that lead to chronic cardiomyopathy.[50] Moreover, the ability of *T. cruzi* to activate NF-κB suggests that NF-κB activation is a determinant of the intracellular survival of *T. cruzi*.[54] One could consider NF-κB as a mechanism triggered by *T. cruzi* to allow the infected host cell to survive. Similarly to other intracellular protozoan parasites, *T. cruzi* subverts the apoptotic machinery to ensure its own survival in the infected cells.[55] NF-κB inhibitors could thus be considered as interesting compounds leading eventually to death of infected host cells thus contributing to a reduced burden of infectious cells in patients. Accordingly, compounds **3** and **4** appear here as the most interesting as they are both potent anti-trypanosomal and anti-NF-κB molecules. Compounds **6** and **12**, probably due to structural specificities, such as the change in the conformation of the macrolide ring due to the double bond in **6** and the planar structure of **12**, inhibit only NF-κB but exhibit no major anti-trypanosomal activity.

3. Experimental section

3.1. General experimental procedures

Optical rotations were determined on a Perkin–Elmer-241 MC polarimeter. ^{1}H and ^{13}C NMR spectra were recorded on Bruker

ARX 500 or AVANCE DMX 600 NMR spectrometers. ESI/MS was conducted on a Finnigan LCQ Deca mass spectrometer. Solvents were distilled before use, and spectral grade solvents were used for spectroscopic measurements. HPLC analysis was performed using a HPLC (Dionex P580) system coupled to a photodiode array detector (UVD340S). Routine detection was at 235, 254, 280, and 340 nm. The separation column (125 × 4 mm, L × ID) was prefilled with Eurospher-10 C18 (Knauer, Germany) using a linear gradient of MeOH and 0.02% H_3PO_4 in H_2O and a flow rate of 1 mL/min. UV data (λ_{max}) for individual compounds were extracted from the on-line UV spectra provided by the instrument software. TLC plates with silica gel F_{254} (Merck, Darmstadt, Germany) were used for monitoring of fractions using EtOAc/MeOH/H_2O (30:5:4) and CH_2Cl_2/MeOH/EtOAc (9:1:0.5 and 8:2:1) solvent systems. Detection was at 254 and 366 nm or by spraying the plates with anisaldehyde reagent.

3.2. Fungal material

3.2.1. Isolation of the fungus

The fungus *Penicillium* sp. (Trichocomaceae) was isolated from fresh healthy stem tissues of *Limonium tubiflorum* (Rutaceae) growing in the wild. The plant was collected in April 2008 near Alexandria, Egypt. A voucher specimen has been deposited at the Department of Pharmacognosy, Faculty of Pharmacy, Alexandria University. The fungal strain was isolated from the stem inner tissues under sterile conditions following an isolation protocol described previously.[29]

3.2.2. Identification of fungal cultures

The fungus was identified using a molecular biological protocol by DNA amplification and sequencing of the ITS region as described previously.[56] The sequence data have been submitted to GenBank, accession number HQ112180. The fungal strain was identified as *Penicillium* sp.; however, due to the lack of similar sequences in GenBank, identification of the strain to the species level was not possible. A voucher strain (strain designation LtSb2) is kept at one of the authors' laboratory (P.P.).

3.3. Cultivation

Mass growth of the fungus for the isolation and identification of new metabolites was carried out in Erlenmeyer flasks (1 L each). The fungus was grown on rice solid medium (to 100 g commercially available rice was added 100 mL of distilled water and kept overnight prior to autoclaving, 10 flasks) at room temperature under static conditions for 30 days.

3.4. Extraction and isolation

Cultures were extracted with EtOAc, and the concentrated residue (10 g) partitioned between *n*-hexane and 90% aqueous MeOH. The 90% aqueous MeOH-soluble material (8 g) was then fractionated by vacuum-liquid chromatography (VLC) on silica gel 60 using *n*-hexane/CH_2Cl_2/MeOH gradient elution. Fractions were then chromatographed over Sephadex LH-20 using MeOH or CH_2Cl_2/MeOH (2:8) as eluting solvents. Further purification was achieved by semi-preparative HPLC (Merck Hitachi L-7100) on an Eurosphere 100-10 C18 column (300 × 8 mm, L × ID, Knauer) using MeOH/H_2O gradient as the mobile phase. Yields of compounds were as follows: **1** 4.5 mg, **2** 1.2 mg, **3** 10.5 mg, **4** 6.7 mg, **5** 1.1 mg, **6** 15.9 mg, **7** 3.3 mg, **8** 3.8 mg, **9** 4.4 mg, **10** 11.6 mg, **11** 3.9 mg, **12** 5.7 mg, **13** 1.2 mg, **14** 2.7 mg, **15** 1.1 mg, and **16** 12.7 mg.

3.4.1. Penilactone (1)

Pale yellow powder; $[\alpha]_D^{20}$ −53 (*c* 0.2, MeOH); UV λ_{max} (PDA) 203.8, 231.5, 284, 321 nm; ^1H and ^{13}C NMR, see Table 1; ESIMS positive *m/z* 305 $[M+H]^+$ (100), 321.9 $[M+NH_4]^+$ (45), 625.6 $[2M+NH_4]^+$ (10), 630.8 $[2M+Na]^+$ (60), negative *m/z* 303 $[M-H]^-$ (100), 606.8 $[2M-H]^-$ (65); HRESIMS *m/z* 306.1078 $[M+H]^+$ (calcd for $C_{16}H_{16}DO_6$, 306.1088).

3.4.2. 10,11-Epoxycurvularin (2)

Yellowish white powder; $[\alpha]_D^{20}$ −82 (*c* 0.2, MeOH); UV λ_{max} (PDA) 221, 238.1, 275, 301.9 nm; ^1H and ^{13}C NMR, see Table 2; ESIMS positive *m/z* 329 $[M+Na]^+$ (100), 634.9 $[2M+Na]^+$ (35), negative *m/z* 305 $[M-H]^-$ (100), 610.8 $[2M-H]^-$ (15); HRESIMS *m/z* 329.0999 $[M+Na]^+$ (calcd for $C_{16}H_{18}O_6Na$, 329.0996).

3.4.3. Neobulgarone G (7)

Dark red powder; $[\alpha]_D^{20}$ −32 (*c* 0.025, acetone); UV λ_{max} (PDA) 227.3, 268.1, 385.2 nm; ^1H and ^{13}C NMR, see Table 3; ESIMS positive *m/z* 304.3 $[C_{16}H_{13}ClO_4]^+$ (100), 320.2 $[C_{16}H_{13}ClO_5]^+$ (70), 622.8 $[M+H]^+$ (30), 645.8 $[M+Na]^+$ (15), negative *m/z* 302.9 $[C_{16}H_{12}ClO_4]^-$ (15), 318.9 $[C_{16}H_{12}ClO_5]^-$ (55), 549.7 $[M-2Cl]^-$ (55), 585.7 $[M-Cl]^-$ (100), 621.2 $[M-H]^-$ (62); HRESIMS *m/z* 623.0866 $[M+H]^+$ (calcd for $C_{32}H_{25}Cl_2O_9$, 623.0870).

3.4.4. Sulfimarine (14)

Yellow viscous residue; UV λ_{max} (PDA) 216.9, 277.4, 313.1 nm; ^1H and ^{13}C NMR, see Table 4; ESIMS positive *m/z* 209.1 $[M+H]^+$ (100), 225.8 $[M+NH_4]^+$ (42), 231.7 $[M+Na]^+$ (37), 438.7 $[2M+Na]^+$ (25); HRESIMS *m/z* 209.0266 $[M+H]^+$ (calcd for $C_{10}H_9O_3S$, 209.0267).

3.5. In vitro antitrypanosomal assay

An Alamar Blue assay was useful in the determination of the in vitro drug sensitivity of African trypanosomes. Stock solution of samples at concentrations of 10 mg/mL or 1 mg/100 μL in DMSO and *Trypanosoma brucei brucei* S427 at concentration of 2–3 × 10^4 trypanosomes/mL were prepared. 20 μg/mL test solutions were prepared by pipetting 4 μL of test stock solution into flat bottomed and transparent 96-well plates and adding 196 μL of HMI-9 medium into each well. Two microliter of 10 μM Suramin in distilled water (filter sterilized) was added to the last column to serve as a positive control. Trypanosomes (100 μL) was eventually added to each well plate then incubated at 37 °C 5% CO_2 with humidified atmosphere for a period of 48 h. Twenty microliters of Alamar Blue was added and the plate was again incubated for 24 h, under the same conditions. The fluorescence was determined using the Wallace Victor apparatus (Exc 530 nmEm 590 nm). Anti-trypanosomal activity was determined using Suramin as a positive control with concentration of 10 μM, and DMSO doubled as both negative control as well as solvent for the screened samples.

3.6. Microculture tetrazolium (MTT) assay

For initial screening the extract was tested for cytotoxicity against L5178Y mouse lymphoma cells using a microculture tetrazolium (MTT) assay and compared to untreated controls as described previously.[57] All experiments were carried out in triplicate and repeated three times. As controls, media with 0.1% EGMME/DMSO were included in the experiments. The depsipeptide kahalalide F isolated from *Elysia grandifolia*[57] was used as positive control.

3.7. Cytotoxic and NF-κB inhibition assays

3.7.1. Cell cultures and reagents

The in vitro growth inhibitory values of the compounds were determined on different cell lines including Human Philadelphia chromosome-positive chronic myelogenous leukemia cells (K562), human T cell leukemia cells (Jurkat) and human histiocytic lymphoma cells (U937). The cell lines were purchased from Deutsche Sammlung für Mikroorganismen und Zellkulturen (DSMZ, Braunschweig, Germany) and cultured in RPMI 1640 medium (Lonza, Verviers, Belgium) supplemented with 10% fetal calf serum (FCS) (Hyclone, Perbio, Erembodegem, Belgium) and 1% (v/v) antibiotic–antimycotic (Lonza, BioWhittaker™, Verviers, Belgium) at 37 °C, in a 5% CO_2, humidified atmosphere. Human recombinant TNFα (PeproTech, Rocky Hill, NJ, USA) was resuspended in a phosphate buffer salt (PBS) 1X sterile solution containing 0.5% bovine serum albumin (MP Biomedicals, Asse-Relegem, Belgium) to reach a final concentration of 10 μg/mL.

3.7.2. In vitro cytotoxic assay (viability assay)

The cell lines were maintained in continuous culture in a humid atmosphere at 37 °C and 5% CO_2 in RPMI 1640 medium supplemented with penicillin, streptomycin, gentamicin, L-glutamine, and fetal calf serum. Potential mycoplasm contaminations were checked twice per month.

For the assay, 24-well plates were seeded with 500 μL of cell suspension containing more or less 2×10^5 cells/mL. Cells were treated with natural compounds at different concentrations (in the range between 0.1 up to 100 μM). After 24 h incubation, the cells were transferred to 96-well microplates and assayed for the CellTiter-Glo® Luminescent Cell Viability Assay to determine the number of viable cells in culture, based on quantification of the ATP present. Each condition was carried out in triplicate. The results correspond to an average of three independent experiments ± SD.

3.7.3. Transient transfections

Transient transfections of K562 cells were performed by electroporation using the BioRad gene Pulser. For each experiment, 3.75×10^6 cells at a concentration of 1.5×10^7 cells/mL were electroporated at the following settings: 250 V and 500 μF. For each transfection, 250 μL of cells were combined with five micrograms of firefly luciferase vector, NF-κB pGL4 (Promega, Leiden, The Netherlands), 5 μg of ph-RG-tk Renilla plasmid (Promega).

After 24 h electroporation, transfected cells were harvested, resuspended in growth medium to reach a final concentration of 10^6 cells/mL and subjected or not to the treatment by 20 ng/mL of TNFα for 6 h. In order to assay Luciferase and Renilla activity, 75 μL Dual-Glo™ Luciferase Reagent (Promega) were incubated for 10 min at 22 °C and then, 75 μL Dual-Glo™ Stop&Glo® Reagent (Promega) were added to the cells for 10 min incubation at 22 °C. Luciferase and Renilla activities were measured with an Orion microplate luminometer (Berthold detection systems) and results are expressed as a ratio of Luciferase activity normalized to Renilla activity.

The IC_{50} value was calculated using a XY scatter dependency chart. The 50% inhibition activity of samples on NF-κB expression was established for each compound separately by using the best fitting trend formulas model. The average value of three independent experiments was applied.

Acknowledgments

Financial support by BMBF (to P.P.) and by MOST (to W.L.) is gratefully acknowledged. B.O. is supported by a doctoral Télévie grant. Research at the Laboratoire de Biologie Moléculaire et Cellulaire du Cancer (LBMCC) is financially supported by the following: 'Recherche Cancer et Sang' foundation, «Recherches Scientifiques Luxembourg» asbl, «Een Häerz fir Kriibskrank Kanner» association, the Action Lions 'Vaincre le Cancer' Luxembourg, The Fonds National de la Recherche Luxembourg, Télévie Luxembourg, the Foundation for Scientific Cooperation between Germany and Luxembourg, the European Union (ITN 'RedCat' 215009 and Interreg IVa project 'Corena').

Supplementary data

Supplementary data associated with this article can be found, in the online version, at doi:10.1016/j.bmc.2010.11.012.

References and notes

1. Overath, P.; Chaudhri, M.; Steverding, D.; Ziegelbauer, K. *Parasitol. Today* **1994**, *10*, 53.
2. Barrett, M. P.; Burchmore, R. J. S.; Stich, A.; Lazzari, J. O.; Frasch, A. C.; Cazzulo, J. J.; Krishna, S. *Lancet* **2003**, *362*, 1469.
3. World Health Organization. *African trypanosomiasis (sleeping sickness)* **2006**, WHO fact sheet number 259.
4. Pikarsky, E.; Porat, R. M.; Stein, I.; Abramovitch, R.; Amit, S.; Kasem, S.; Gutkovich-Pyest, E.; Urieli-Shoval, S.; Galun, E.; Ben-Neriah, Y. *Nature* **2004**, *431*, 461.
5. Karin, M.; Greten, F. R. *Nat. Rev. Immunol.* **2005**, *5*, 749.
6. Kempe, S.; Kestler, H.; Lasar, A.; Wirth, T. *Nucleic Acids Res.* **2005**, *33*, 5308.
7. Cárcamo, J. M.; Pedraza, A.; Bórquez-Ojeda, O.; Golde, D. W. *Biochemistry* **2002**, *41*, 12995.
8. Ghosh, S.; Karin, M. *Cell* **2002**, *109*, S81.
9. Karin, M.; Cao, Y.; Greten, F. R.; Li, Z. W. *Nat. Rev. Cancer* **2002**, *2*, 301.
10. Houghton, J.; Stoicov, C.; Nomura, S.; Rogers, A. B.; Carlson, J.; Li, H.; Cai, X.; Fox, J. G.; Goldenring, J. R.; Wang, T. C. *Science* **2004**, *306*, 1568.
11. Bharti, A. C.; Aggarwal, B. B. *Ann. N. Y. Acad. Sci.* **2002**, *973*, 392.
12. Aly, A. H.; Debbab, A.; Kjer, J.; Proksch, P. *Fungal Divers.* **2010**, *41*, 1.
13. Debbab, A.; Aly, A. H.; Lin, W. H.; Proksch, P. *Microb. Biotechnol.* **2010**, *3*, 544.
14. Zhang, H. W.; Song, Y. C.; Tan, R. X. *Nat. Prod. Rep.* **2006**, *23*, 753.
15. Bacon, C. W.; White, J. F. *Microbial Endophytes*; Marcel Dekker: New York, 2000. pp 341–388.
16. Redman, R. S.; Sheehan, K. B.; Stout, T. G.; Rodriguez, R. J.; Henson, J. M. *Science* **2002**, *298*, 1581.
17. Bae, H.; Sicher, R. C.; Kim, M. S.; Kim, S. H.; Strem, M. D.; Melnick, R. L.; Bailey, B. A. *J. Exp. Bot.* **2009**, *60*, 3279.
18. Giordano, L.; Gonthier, P.; Varese, G. C.; Miserere, L.; Nicolotti, G. *Fungal Divers.* **2009**, *38*, 69.
19. Brady, S. F.; Bondi, S. M.; Clardy, J. *J. Am. Chem. Soc.* **2001**, *123*, 9900.
20. Strobel, G. A.; Miller, R. V.; Miller, C.; Condron, M.; Teplow, D. B.; Hess, W. M. *Microbiology* **1999**, *145*, 1919.
21. Strobel, G. A. *Can. J. Plant Pathol.* **2002**, *24*, 14.
22. Lingham, R. B.; Silverman, K. C.; Bills, G. F.; Cascales, C.; Sanchez, M.; Jankins, R. G.; Gartner, S. E.; Martin, I.; Diez, M. T.; Pelaez, F.; Mochales, S.; Kong, Y.-L.; Burg, R. W.; Meinz, M. S.; Huang, L.; Nallin-Omstead, M.; Mosser, S. D.; Schaber, M. D.; Omer, C. A.; Pompliano, D. L.; Gibbs, J. B.; Singh, S. B. *Appl. Microbiol. Biotechnol.* **1993**, *40*, 370.
23. Li, J. Y.; Strobel, G. A.; Harper, J. K.; Lobkovsky, E.; Clardy, J. *Org. Lett.* **2000**, *2*, 767.
24. Strobel, G.; Daisy, B. *Microbiol. Mol. Biol. Rev.* **2003**, *67*, 491.
25. Larsen, T. O.; Smedsgaard, J.; Nielsen, K. F.; Hansen, M. E.; Frisvad, J. C. *Nat. Prod. Rep.* **2005**, *22*, 672.
26. Aly, A. H.; Debbab, A.; Edrada-Ebel, R. A.; Müller, W. E. G.; Kubbutat, M. H. G.; Wray, V.; Ebel, R.; Proksch, P. *Mycosphere* **2010**, *1*, 153.
27. Debbab, A.; Aly, A. H.; Edrada-Ebel, R. A.; Wray, V.; Müller, W. E. G.; Totzke, F.; Zirrgiebel, U.; Schächtele, C.; Kubbutat, M. H. G.; Lin, W. H.; Mosaddak, M.; Hakiki, A.; Proksch, P.; Ebel, R. *J. Nat. Prod.* **2009**, *72*, 626.
28. Kjer, J.; Wray, V.; Edrada-Ebel, R.; Ebel, R.; Pretsch, A.; Lin, W. H.; Proksch, P. *J. Nat. Prod.* **2009**, *72*, 2053.
29. Aly, A. H.; Edrada-Ebel, R. A.; Indriani, I. D.; Wray, V.; Müller, W. E. G.; Totzke, F.; Zirrgiebel, U.; Schächtele, C.; Kubbutat, M. H. G.; Lin, W. H.; Proksch, P.; Ebel, R. *J. Nat. Prod.* **2008**, *71*, 972.
30. Munro, H. D.; Musgrave, O. C.; Templeton, R. *J. Chem. Soc. C* **1967**, 947.
31. Lai, S.; Shizuri, Y.; Yamamura, S.; Kawai, K.; Terada, Y.; Furukawa, H. *Tetrahedron Lett.* **1989**, *30*, 2241.
32. Ghisalberti, E. L.; Hockless, D. C. R.; Rowland, C. Y.; White, A. H. *Aust. J. Chem.* **1993**, *46*, 571.
33. Greve, H.; Schupp, P. J.; Eguereva, E.; Kehraus, S.; Kelter, G.; Maier, A.; Fiebig, H.-H.; König, G. M. *Eur. J. Org. Chem.* **2008**, 5085.
34. Hussain, H.; Akhtar, N.; Draeger, S.; Schulz, B.; Pescitelli, G.; Salvadori, P.; Antus, S.; Kurtán, T.; Krohn, K. *Eur. J. Org. Chem.* **2009**, 749.
35. Eilbert, F.; Anke, H.; Sterner, O. *J. Antibiot.* **2000**, *53*, 1123.
36. Mbwambo, Z. H.; Apers, S.; Moshi, M. J.; Kapingu, M. C.; Van Miert, S.; Claeys, M.; Brun, R.; Cos, P.; Pieters, L.; Vlietinck, A. *Planta Med.* **2004**, *70*, 706.

37. Ndjakou Lenta, B.; Devkota, K. P.; Ngouela, S.; Fekam Boyom, F.; Naz, Q.; Choudhary, M. I.; Tsamo, E.; Rosenthal, P. J.; Sewald, N. *Chem. Pharm. Bull.* **2008**, *56*, 222.
38. Joseph-Nathan, P.; Domínguez, M.; Ortega, D. A. *J. Heterocycl. Chem.* **1984**, *21*, 1141.
39. Fugmann, B.; Arnold, S.; Steglich, W.; Fleischhauer, J.; Repges, C.; Koslowski, A.; Raabe, G. *Eur. J. Org. Chem.* **2001**, 3097.
40. Günther, H.; Prestien, J.; Joseph-Nathan, P. *Org. Magn. Reson.* **1975**, *7*, 339.
41. Clennan, E. L.; Yang, K. *J. Org. Chem.* **1992**, *57*, 4477.
42. Patil, A. D.; Freyer, A. J.; Killmer, L.; Zuber, G.; Carte, B.; Jurewicz, A. J.; Johnson, R. K. *Nat. Prod. Lett.* **1997**, *10*, 225.
43. Liang, Q.; Sun, Y.; Yu, B.; She, X.; Pan, X. *J. Org. Chem.* **2007**, *72*, 9846.
44. Fujimoto, H.; Nakamura, E.; Okuyama, E.; Ishibashi, M. *Chem. Pharm. Bull.* **2004**, *52*, 1005.
45. Cohen, P. A.; Neil Towers, G. H. *Phytochemistry* **1996**, *42*, 1325.
46. Ayer, W. A.; Trifonov, L. S. *J. Nat. Prod.* **1994**, *57*, 317.
47. Kashiwada, Y.; Nonaka, G.-I.; Nishioka, I. *Chem. Pharm. Bull.* **1984**, *32*, 3493.
48. Andrade, R.; Ayer, W. A.; Mebe, P. P. *Can. J. Chem.* **1992**, *70*, 2526.
49. He, J.; Wijeratne, E. M.; Bashyal, B. P.; Zhan, J.; Seliga, C. J.; Liu, M. X.; Pierson, E. E., ; Pierson, L. S., 3rd; VanEtten, H. D.; Gunatilaka, A. A. *J. Nat. Prod.* **2004**, *67*, 1985.
50. Huang, H.; Calderon, T. M.; Berman, J. W.; Braunstein, V. L.; Weiss, L. M.; Wittner, M.; Tanowitz, H. B. *Infect. Immun.* **1999**, *67*, 5434.
51. Ba, X.; Gupta, S.; Davidson, M.; Garg, N. J. *J. Biol. Chem.* **2010**, *285*, 11596.
52. Huang, H.; Petkova, S. B.; Cohen, A. W.; Bouzahzah, B.; Chan, J.; Zhou, J. N.; Factor, S. M.; Weiss, L. M.; Krishnamachary, M.; Mukherjee, S.; Wittner, M.; Kitsis, R. N.; Pestell, R. G.; Lisanti, M. P.; Albanese, C.; Tanowitz, H. B. *Infect. Immun.* **2003**, *71*, 2859.
53. Bergeron, M.; Olivier, M. *J. Immunol.* **2006**, *177*, 6271.
54. Hall, B. S.; Tam, W.; Sen, R.; Pereira, M. E. *Mol. Biol. Cell* **2000**, *11*, 153.
55. Heussler, V. T.; Küenzi, P.; Rottenberg, S. *Int. J. Parasitol.* **2001**, *31*, 1166.
56. Wang, S.; Li, X. M.; Teuscher, F.; Li, D. L.; Diesel, A.; Ebel, R.; Proksch, P.; Wang, B. G. *J. Nat. Prod.* **2006**, *69*, 1622.
57. Ashour, M.; Edrada, R. A.; Ebel, R.; Wray, V.; Wätjen, W.; Padmakumar, K.; Müller, W. E. G.; Lin, W. H.; Proksch, P. *J. Nat. Prod.* **2006**, *69*, 1547.